AIAA Guidance, Navigation, and Control Conference
08 - 11 August 2011, Portland, Oregon

Adaptive Estimation Based Loss of Control Detection and Mitigation

Vahram Stepanyan *
Mission Critical Technologies Inc, NASA Ames Research Center, Moffett Field, CA 94035,
Kalmanje Krishnakumar †
NASA Ames Research Center, Moffett Field, CA 94035,
Jonathan Barlow ‡
Stinger Ghaffarian Technologies Inc., NASA Ames Research Center, Moffett Field, CA 94035,
Hildo Bijl §
Delft University of Technology, Delft, Netherlands

Aircraft loss-of-control (LOC) is a significant contributor to accidents and fatalities across all vehicle classes and phases of flight, and has been the subject of several studies. LOC events are usually precipitated by an adverse onboard condition or an external hazard or disturbance leading to a deficiency in the control inputs needed to counteract the adverse event. The paper presents an approach using an adaptive prediction method to identify in real-time the control deficiency to counteract the adverse condition. This deficiency signal can either be used to provide a feedback to the pilot (via a tactile, aural and/or visual feedback) or to augment the existing control signal to keep the aircraft stable. We document results and its efficacy using the NASA Generic Transport Model that simulates typical adverse conditions.

I. Introduction

Aircraft system faults, failures, and errors are the leading initial factors in many LOC events.[1] Inappropriate crew response is the second most likely initial event that leads to such events. This is due to the fact that flying near the edge of a safe operating envelope is an inherently unsafe proposition. Edge of the envelope here implies that small changes or disturbances in system state or system dynamics can take the system out of the safe envelope in a short time and could result in catastrophic failures. Performance that fully exploits available resources to maintain safe flight in the midst of either greater uncertainty or greater needed performance than originally planned is non trivial.

Quantitative measures of the LOC events are proposed in Ref.[12] in the form of five envelopes in the two dimensional parameter space. When the aircraft dynamics is known, the analysis of the effects of nonlinearities on the LOC are provided in Ref.,[4] and the estimation of the region of attraction around a trim point is provided in Ref.[8] However, the real-time estimation of the envelope boundaries for the uncertain aircraft is not an easy task. It requires some form of online identification, which in turn requires special maneuvers to provide sufficiently rich signals necessary for the parameter convergence. Examples of online identifications include but are not limited to application of the dual unscented Kalman filter,[5] two-stage extended Kalman filter,[9] Fourier Transform Regression,[6] adaptive estimation,[11] etc.

In this paper, we outline a novel approach to the detection and mitigation of LOC situation by providing a control deficiency needed to keep the aircraft within the safe envelope. Real-time assessment and prediction

*Senior Scientist, Mission Critical Technologies Inc., Senior Member AIAA, vahram.stepanyan@nasa.gov
†Group Lead, Adaptive Control and Evolvable Systems, Intelligent Systems Division, Associate Fellow AIAA, kalmanje.krishnakumar@nasa.gov
‡Research Scientist, Stinger Ghaffarian Technologies Inc., jonathan.s.barlow@nasa.gov
§Graduate student, Department of Aerospace Engineering, hildobijl@gmail.com

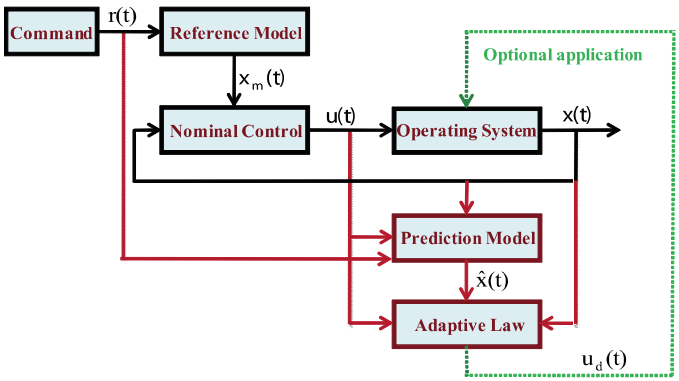

Figure 1. The schematics of the system with the prediction model.

of flight control deficiency to counteract the adverse conditions will provide a key capability in providing improved onboard situational awareness to the pilot and options for adaptive control for aircraft recovery. The novel control framework uses an adaptive prediction method, which works parallel to the flight control system without interacting with it. It takes the aircraft's input and state measurement signals to generate the adaptive estimates of the unknown parameters. Unlike the traditional identification methods, it does not require parameter convergence, hence there is no need for the special maneuvers. In traditional model reference adaptive control, a closed loop controller is designed with adaptable controller parameters or gains. The output of the system is compared to a desired response from a reference model. The control parameters are update based on this error. As the adaptation converges, the plant model closely matches the reference model response. In our approach (See Figure 1), a predicted model is used to derive adaptive control signals that are compared with the aircraft control signals to estimate a control deficiency. This deficiency can be either used to make the system control the aircraft to keep it within the safe envelope or provide the feedback to the pilot to improve the situational awareness.

In the rest of the paper, we present details of the adaptive prediction concept and present simulation study results using the NASA Generic Transport model that enables high-fidelity simulation of certain adverse conditions.

II. Nominal System

The nominal aircraft's inner-loop dynamics is given by the equation

$$J_0\dot{\boldsymbol{\omega}}(t) + \boldsymbol{\omega}(t) \times J_0\boldsymbol{\omega}(t) = \boldsymbol{m}(\boldsymbol{\omega}, \boldsymbol{\sigma})\,, \tag{1}$$

where J_0 is the nominal inertia matrix, $\boldsymbol{\omega} = [p\ q\ r]^\top$ is the aircraft's angular rate, $\boldsymbol{\sigma} = [1\ \alpha\ \beta\ M\ \dot{\alpha}]^\top$ represents the outer-loop variables and the effect of trim conditions, and $\boldsymbol{m}(\boldsymbol{\omega}, \boldsymbol{\sigma})$ is the aerodynamic moment, which is assumed to be linear in its variables at nominal flight conditions. Expressing the term $J_0^{-1}\boldsymbol{\omega}(t) \times J_0\boldsymbol{\omega}(t)$ as a linear parametric form $W_0\boldsymbol{g}(\boldsymbol{\omega})$, where $\boldsymbol{g}(\boldsymbol{\omega}) = [p^2\ q^2\ r^2\ pq\ qr\ pr]^\top$, the inner-loop dynamics can be represented in the form

$$\dot{\boldsymbol{\omega}}(t) = W_0\boldsymbol{g}(\boldsymbol{\omega}) + A_0\boldsymbol{\omega}(t) + G_0\boldsymbol{\sigma}(t) + B_0\boldsymbol{u}(t)\,, \tag{2}$$

where $\boldsymbol{u} = [\delta_a\ \delta_e\ \delta_r]^\top$ is the control input, $A_0 \in R^{3\times3}$, $G_0 \in R^{3\times5}$ and $B_0 \in R^{3\times3}$ are constant matrices representing the stability and control derivatives.

We assume that for the nominal aircraft a dynamic inversion flight control is designed such that the angular rate vector $\boldsymbol{\omega}(t)$ tracks the output $\boldsymbol{\omega}_m(t)$ of a reference model, driven by the pilot's command $\boldsymbol{\omega}_c(t)$, which is assumed to be smooth and bounded with a bounded integral. The reference model has the form

$$\dot{\boldsymbol{\omega}}_m(t) = -K_p[\boldsymbol{\omega}_m(t) - \boldsymbol{\omega}_c(t)] - K_i\int_0^t [\boldsymbol{\omega}_m(\tau) - \boldsymbol{\omega}_c(\tau)]d\tau\,, \tag{3}$$

where $K_p = diag\,(k_{p,1}, k_{p,2}, k_{p,3})$ and $K_i = diag\,(k_{i,1}, k_{i,2}, k_{i,3})$ are the proportional and integral gains chosen for the reference model to satisfy the performance specifications and provide good handling qualities. In

particular, we set $k_{i,j} = \omega_j^2$ and $k_{p,j} = 2\zeta_i\omega_j$, where ω_j and ζ_j represents the frequency and the damping ratio of the j-th channel. The nominal control has the form

$$\boldsymbol{u}_0(t) = B_0^{-1}\left[-W_0\boldsymbol{g}(\boldsymbol{\omega}) - A_0\boldsymbol{\omega}(t) - G_0\boldsymbol{\sigma}(t) + \dot{\boldsymbol{\omega}}_d(t)\right], \tag{4}$$

where $\dot{\boldsymbol{\omega}}_d(t)$ is the desired angular acceleration given by

$$\dot{\boldsymbol{\omega}}_d(t) = -K_p[\boldsymbol{\omega}(t) - \boldsymbol{\omega}_m(t)] - K_i\int_0^t[\boldsymbol{\omega}(\tau) - \boldsymbol{\omega}_m(\tau)]d\tau + \dot{\boldsymbol{\omega}}_m(t)\,. \tag{5}$$

Denoting the tracking error by $\boldsymbol{e}_\omega = \boldsymbol{\omega} - \boldsymbol{\omega}_m$, it is easy to see that the error dynamics reduce to the exponentially stable system

$$\dot{\boldsymbol{e}}(t) = A_m\boldsymbol{e}(t)\,, \tag{6}$$

where

$$\boldsymbol{e}(t) = \begin{bmatrix} \int_0^t \boldsymbol{e}_\omega(\tau)d\tau \\ \boldsymbol{e}_\omega(t) \end{bmatrix},\ A_m = \begin{bmatrix} 0_{3\times3} & \mathbb{I}_{3\times3} \\ -K_i & -K_p \end{bmatrix}.$$

We immediately notice that for a given positive definite symmetric matrix Q there exists a positive definite symmetric matrix P satisfying the Lyapunov equation

$$A_m^\top P + PA_m = -Q\,. \tag{7}$$

III. Adaptive Prediction Model

Under the off-nominal conditions the aircraft dynamics can be described by the equation

$$\dot{\boldsymbol{\omega}}(t) = W\boldsymbol{g}(\boldsymbol{\omega}) + A\boldsymbol{\omega}(t) + G\boldsymbol{\sigma}(t) + B\boldsymbol{u}(t) + U\boldsymbol{\phi}(\boldsymbol{\omega},\boldsymbol{\sigma})\,, \tag{8}$$

where $W = W_0 + \Delta W$, $A = A_0 + \Delta A$, $G = G_0 + \Delta G$, $B = B_0 + \Delta B$, and U are unknown constant matrices representing the system's uncertainties. The last term has been introduced to represent the possible nonlinearities in the expression of the aerodynamic moment under the off-nominal conditions, and is assumed to be linearly parameterized. Assuming that the system still operates with the nominal controller $\boldsymbol{u}(t) = \boldsymbol{u}_0(t)$, the error dynamics take the form

$$\dot{\boldsymbol{e}}(t) = A_m\boldsymbol{e}(t) + B_m\Theta\boldsymbol{f}(\boldsymbol{\omega},\boldsymbol{\sigma})\,, \tag{9}$$

where we denote

$$B_m = \begin{bmatrix} 0_{3\times3} \\ \mathbb{I}_{3\times3} \end{bmatrix}, \Theta = \begin{bmatrix} \Delta W & \Delta A & \Delta G & \Delta B & U \end{bmatrix}, \quad \boldsymbol{f}(\boldsymbol{\omega},\boldsymbol{\sigma}) = \begin{bmatrix} \boldsymbol{g}(\boldsymbol{\omega}) \\ \boldsymbol{\omega} \\ \boldsymbol{\sigma} \\ \boldsymbol{u} \\ \boldsymbol{\phi}(\boldsymbol{\omega},\boldsymbol{\sigma}) \end{bmatrix}.$$

Obviously, $\Theta = 0$ for the nominal system.

In order to detect the anomalies in the system we introduce an adaptive prediction model for the error dynamics as follows

$$\begin{aligned} \dot{\hat{\boldsymbol{e}}}(t) &= A_m\hat{\boldsymbol{e}}(t) + B_m\hat{\Theta}(t)\boldsymbol{f}(\boldsymbol{\omega},\boldsymbol{\sigma}) + \lambda\tilde{\boldsymbol{e}}(t) \\ \dot{\hat{\boldsymbol{e}}}_\omega(t) &= C_m\dot{\hat{\boldsymbol{e}}}(t)\,, \end{aligned} \tag{10}$$

where $\hat{\boldsymbol{e}}(t)$ is the prediction of the error signal $\boldsymbol{e}(t)$, $C_m = [0_{3\times3}\ \mathbb{I}_{3\times3}]$, $\hat{\boldsymbol{e}}_\omega(t)$ is the prediction of the tracking error, $\tilde{\boldsymbol{e}}(t) = \boldsymbol{e}(t) - \hat{\boldsymbol{e}}(t)$ is the prediction error, $\lambda > 0$ is a design parameter, $\hat{\Theta}(t)$ is the parameter estimate generated online according to the adaptive law

$$\dot{\hat{\Theta}}(t) = \gamma\boldsymbol{f}(\boldsymbol{\omega},\boldsymbol{\sigma})\tilde{\boldsymbol{e}}^\top(t)PB_m\,, \tag{11}$$

where $\gamma > 0$ is the adaptation rate. Clearly, the prediction error $\tilde{\boldsymbol{e}}(t)$ satisfies the dynamic equation

$$\dot{\tilde{\boldsymbol{e}}}(t) = (A_m - \lambda \mathbb{I}_{6\times 6})\tilde{\boldsymbol{e}}(t) + B_m \tilde{\Theta}(t)\boldsymbol{f}(\boldsymbol{\omega}, \boldsymbol{\sigma})\,, \tag{12}$$

where $\tilde{\Theta}(t) = \Theta - \hat{\Theta}(t)$ is the parameter estimation error. The prediction of the state is readily constructed from the error estimate as $\hat{\boldsymbol{\omega}}(t) = \boldsymbol{\omega}_m(t) + \hat{\boldsymbol{e}}_\omega(t)$. On the other hand, it can be generated by the dynamic equation

$$\dot{\hat{\boldsymbol{\omega}}}(t) = -K_p[\hat{\boldsymbol{\omega}}(t) - \boldsymbol{\omega}(t)] - K_i \int_0^t [\hat{\boldsymbol{\omega}}(\tau) - \boldsymbol{\omega}(\tau)]d\tau + B_0\boldsymbol{u}(t) + \hat{\Theta}(t)\boldsymbol{f}(\boldsymbol{\omega}, \boldsymbol{\sigma}) + \lambda\tilde{\boldsymbol{\omega}}(t)\,, \tag{13}$$

where $\tilde{\boldsymbol{\omega}}(t) = \boldsymbol{\omega}(t) - \hat{\boldsymbol{\omega}}(t)$ is the state prediction error, and is identical with the error signal $C_m\tilde{\boldsymbol{e}}(t)$, since

$$\boldsymbol{\omega}(t) - \hat{\boldsymbol{\omega}}(t) = (\boldsymbol{\omega}_m(t) + \boldsymbol{e}_\omega(t)) - (\boldsymbol{\omega}_m(t) + \hat{\boldsymbol{e}}_\omega(t)) = \tilde{\boldsymbol{e}}_\omega(t) = C_m\tilde{\boldsymbol{e}}(t)\,. \tag{14}$$

Therefore, the properties of the state prediction signal $\hat{\boldsymbol{\omega}}(t)$ can be investigated via the error prediction $\hat{\boldsymbol{e}}(t)$, whose dynamics are more suitable for the analysis.

IV. Control Deficiency Signal

It can be observed from the error dynamics (9) that the tracking error $\boldsymbol{e}(t)$ cannot converge to zero in the presence of nonzero uncertainty $\Theta\boldsymbol{f}(\boldsymbol{\omega}, \boldsymbol{\sigma})$, when the system operates under the nominal control law. That is, the controller is missing the signal $\boldsymbol{u}_a(t) = B_0^{-1}\Theta\boldsymbol{f}(\boldsymbol{\omega}, \boldsymbol{\sigma})$ needed to provide the required performance. From this point of view $\boldsymbol{u}_a(t)$ is called the control deficiency. Since Θ is unknown, $\boldsymbol{u}_a(t)$ is inaccessible. However, its estimate $\hat{\boldsymbol{u}}_a(t) = B_0^{-1}\hat{\Theta}(t)\boldsymbol{f}(\boldsymbol{\omega}, \boldsymbol{\sigma})$ can be readily computed, which can be used to detect the loss-of-control situation. As it is shown in the next section, $\hat{\boldsymbol{u}}_a(t)$ closely follows $\boldsymbol{u}_a(t)$ not only on steady state, but also in transient. Therefore, a nonzero signal $\hat{\boldsymbol{u}}_a(t)$ (or when $\hat{\boldsymbol{u}}_a(t)$ exceeds a given threshold) alerts the pilot about the emergency.

Obviously if we close the loop with the adaptive augmentation $\hat{\boldsymbol{u}}_a(t) = B_0^{-1}\hat{\Theta}(t)\boldsymbol{f}(\boldsymbol{\omega}, \boldsymbol{\sigma})$, that is if we set

$$\boldsymbol{u}(t) = \boldsymbol{u}_0(t) + \hat{\boldsymbol{u}}_a(t)\,, \tag{15}$$

the tracking error dynamics take the form

$$\dot{\boldsymbol{e}}(t) = A_m\boldsymbol{e}(t) + B_m\tilde{\Theta}(t)\boldsymbol{f}(\boldsymbol{\omega}, \boldsymbol{\sigma})\,, \tag{16}$$

which means that the tracking error can still converge to zero when the term $\tilde{\Theta}(t)\boldsymbol{f}(\boldsymbol{\omega}, \boldsymbol{\sigma})$ converges to zero.

When the estimate of the control deficiency signal is applied to the system, the state prediction dynamics (13) reduce to the system

$$\dot{\hat{\boldsymbol{\omega}}}(t) = -K_p[\hat{\boldsymbol{\omega}}(t) - \boldsymbol{\omega}_c(t)] - K_i \int_0^t [\hat{\boldsymbol{\omega}}(\tau) - \boldsymbol{\omega}_c(\tau)]d\tau + \lambda\tilde{\boldsymbol{\omega}}(t)\,, \tag{17}$$

which is in the form of the modified reference model as in the Ref.[10] Therefore, the analysis methods of the M-MRAC (Modified Reference Model MRAC) architecture can be applied here as well. This is done in the next section, where we show that the adaptive signals have nice transient and steady state properties, which makes the control deficiency signal an attractive option for the pilots to use in the closed-loop in loss-of control situations. The schematics of the estimation algorithm with an optional control path is shown in Figure 1.

We notice that closing the loop with the estimate of the control deficiency signal generates an algebraic loop in the control definition, which can be written in the expanded form as

$$\boldsymbol{u}(t) = \boldsymbol{u}_0(t) - B_0^{-1}\left[\Delta\hat{W}(t)\boldsymbol{g}(\boldsymbol{\omega}) + \hat{\Delta A}(t)\boldsymbol{\omega}(t) + \hat{\Delta A}(t)\boldsymbol{\sigma}(t) + \hat{\Delta B}(t)\boldsymbol{u}(t) + \hat{U}(t)\boldsymbol{\phi}(\boldsymbol{\omega}, \boldsymbol{\sigma})\right]. \tag{18}$$

Solving the equation (18) for $\boldsymbol{u}(t)$ we obtain

$$\left[B_0 + \hat{\Delta B}(t)\right]\boldsymbol{u}(t) = B_0\boldsymbol{u}_0(t) - \Delta\hat{W}(t)\boldsymbol{g}(\boldsymbol{\omega}) - \hat{\Delta A}(t)\boldsymbol{\omega}(t) - \hat{\Delta A}(t)\boldsymbol{\sigma}(t)\boldsymbol{u}(t) - \hat{U}(t)\boldsymbol{\phi}(\boldsymbol{\omega}, \boldsymbol{\sigma})\,, \tag{19}$$

implying that the algebraic loop is solvable if the matrix $\hat{B}(t) = B_0 + \hat{\Delta B}(t)$ is non-singular. Since the uncertain matrix b is usually non-singular, the adaptive law for the estimate of ΔB can be defined by means of the projection operator to provide the non-singularity of matrix $\hat{B}(t)$. However, this requires a priori knowledge of the bounds on the entries of matrix B, which are available in most situations.

V. Analysis of Adaptive Signals

In this section, we analyze the asymptotic and transient properties of the estimates signals. The following lemma presents the asymptotic properties.

Lemma V.1 *Consider the error system (9) and the prediction model (10) along with the adaptive law (11). If $\boldsymbol{e}(t)$ remains bounded, then the following asymptotic relationships hold*

$$\begin{aligned} \hat{\boldsymbol{e}}(t) &\rightarrow \boldsymbol{e}(t) && (20)\\ \dot{\hat{\boldsymbol{e}}}(t) &\rightarrow \dot{\boldsymbol{e}}(t) && (21)\\ \hat{\Theta}(t)\boldsymbol{g}(\boldsymbol{x},\boldsymbol{r}) &\rightarrow \Theta\boldsymbol{g}(\boldsymbol{x},\boldsymbol{r})\,. && (22) \end{aligned}$$

as $t \rightarrow \infty$.

Proof. Consider the following candidate Lyapunov function

$$V(t) = \tilde{\boldsymbol{e}}^\top(t)P\tilde{\boldsymbol{e}}^\top(t) + \frac{1}{\gamma}\mathrm{tr}\left(\tilde{\Theta}^\top(t)\tilde{\Lambda}\Theta(t)\right)\,.$$

Its derivative can be readily computed to be

$$\dot{V}(t) = -\tilde{\boldsymbol{e}}^\top(t)Q\tilde{\boldsymbol{e}}(t) - 2\lambda\tilde{\boldsymbol{e}}^\top(t)P\tilde{\boldsymbol{e}}(t) + 2\mathrm{tr}\left(\tilde{\Theta}^\top(t)\left[\boldsymbol{f}(\boldsymbol{\omega},\boldsymbol{\sigma})\tilde{\boldsymbol{e}}^\top(t)PB_m + \frac{1}{\gamma}\dot{\tilde{\Theta}}^\top(t)\right]\right)\,. \quad (23)$$

Since $\dot{\tilde{\Theta}}(t) = -\dot{\hat{\Theta}}(t)$, substituting the adaptive laws results in

$$\dot{V}(t) = -\tilde{\boldsymbol{e}}^\top(t)Q\tilde{\boldsymbol{e}}^\top(t) - 2\lambda\tilde{\boldsymbol{e}}^\top(t)P\tilde{\boldsymbol{e}}^\top(t)\,, \quad (24)$$

which implies that the error signals $\tilde{\boldsymbol{e}}(t)$ and $\tilde{\Theta}(t)$ are globally stable. On the other hand, if $\boldsymbol{e}(t)$ is bounded, then $\hat{\boldsymbol{\omega}}(t)$, $\boldsymbol{\omega}(t)$, $\int_0^t \hat{\boldsymbol{\omega}}(\tau)d\tau$ and $\int_0^t \boldsymbol{\omega}(\tau)d\tau$ are bounded, implying that $\boldsymbol{u}_0(t)$ and $\boldsymbol{f}(\boldsymbol{\omega},\boldsymbol{\sigma})$ are bounded as well (it is assumed that the outer-loop variables are kept bounded by the pilot's input when the inner-loop variables are bounded). That is, all closed-loop signals are bounded. Therefore, from the prediction error dynamics (12) it follows that $\dot{\tilde{\boldsymbol{e}}}(t)$ is bounded. Application of the Barbalat's lemma[3] results in the limit (20). Further, $\ddot{\tilde{\boldsymbol{e}}}(t)$ can be shown to be bounded by differentiation of the error system (12) and by taking into account the boundedness of the the closed loop signals. Therefore, $\dot{\tilde{\boldsymbol{e}}}(t)$ is uniformly continuous (it has a bounded derivative). Since it has a finite integral $\tilde{\boldsymbol{e}}(t)$, it follows from the Barbalat's lemma that $\dot{\tilde{\boldsymbol{e}}}(t) \rightarrow 0$ as $t \rightarrow \infty$, which proves (21). The last limit follows from the first two and the prediction error dynamics (12). □

Lemma V.1 states that the prediction error is stable for any initial conditions. However, the asymptotic prediction is guaranteed when the state of the operating aircraft remains bounded. The next lemma shows that the prediction error bounds can be decreased as desired by increasing the adaptation rate without assuming the boundedness of the operating system.

Lemma V.2 *Consider the system (9) and the prediction model (10) along with the adaptive law (11). The following bounds are true*

$$\begin{aligned} \|\tilde{\boldsymbol{e}}(t)\|_{\mathcal{L}_\infty} &\leq \frac{c_1}{\sqrt{\gamma}} && (25)\\ \|\tilde{\boldsymbol{e}}(t)\|_{\mathcal{L}_2} &\leq \frac{c_2}{\sqrt{\gamma}}\,, && (26) \end{aligned}$$

where c_1 and c_2 are positive constants.

Proof. Lemma V.1 assures that the Lyapunov function $V(t)$ is non-increasing. Therefore, the following relationships hold

$$\lambda_{\min}(P)\|\tilde{\boldsymbol{e}}(t)\|^2 \leq V(t) \leq V(0)\,, \quad (27)$$

where $\lambda_{\min}(P)$ denotes the minimum eigenvalue of matrix P. Since the prediction model can be initialized such that $\tilde{\boldsymbol{e}}(0) = 0$, we can write

$$\|\tilde{\boldsymbol{e}}(t)\| \leq \frac{\mu}{\sqrt{\lambda_{\min}(P)}\sqrt{\gamma}}\,, \tag{28}$$

where the positive constant μ is defined as

$$\mu = \sqrt{\mathrm{tr}\left(\tilde{\Theta}(0)\tilde{\Theta}^{\top}(0)\right)}\,. \tag{29}$$

Since the inequality (28) holds uniformly in t we conclude that (25) is true with $c_1 = \frac{\mu}{\sqrt{\lambda_{\min}(P)}}$.

On the other hand, integrating the equation (24) and taking into account positive definiteness of $V(t)$ we obtain

$$[\lambda_{\min}(Q) + 2\lambda\lambda_{\min}(P)] \int_0^t \|\tilde{\boldsymbol{e}}(\tau)\|^2 d\tau \leq V(0)\,, \tag{30}$$

which implies the bound (25) with

$$c_2 = \frac{\mu}{\sqrt{\lambda_{\min}(Q) + 2\lambda\lambda_{\min}(P)}}.$$

□

From the derived norm bounds in (25) and (26) it follows that the error signal $\tilde{\boldsymbol{e}}(t)$ can be arbitrarily decreased by increasing the adaptation rate γ. Therefore, a satisfactory prediction can be obtained even for the unstable aircraft.

One of our objectives is to provide an on-demand cue to the pilot in a loss-of-control situation. One of this type of cues is the estimate of the control deficiency, which can be plugged into the closed loop operating system as a recovery option.

It follows from Lemma V.1 that when $\boldsymbol{u}(t) = \boldsymbol{u}_0(t) + \hat{\boldsymbol{u}}_a(t)$ is applied to the uncertain aircraft and the prediction model, then $\hat{\Theta}(t)\boldsymbol{f}(\boldsymbol{\omega}, \boldsymbol{\sigma}) \to \Theta\boldsymbol{f}(\boldsymbol{\omega}, \boldsymbol{\sigma})$. Therefore, $\hat{\boldsymbol{u}}_a(t)$ converges to its ideal value $\boldsymbol{u}_a(t)$. The next lemma shows that with the presented algorithm the adaptive signal $\hat{\boldsymbol{u}}_a(t)$ cannot exhibit large excursions or high frequency oscillations, unlike the conventional adaptive estimation methods.

Lemma V.3 *Consider the system (9) and the prediction model (10) along with the adaptive law (11). If $\boldsymbol{e}(t)$ is bounded, then the inequality*

$$\|\boldsymbol{\eta}(t)\| \leq c_3 e^{-\nu t} + \frac{c_4}{\sqrt{\gamma}} \tag{31}$$

holds, where $\boldsymbol{\eta}(t) = B_0\tilde{\boldsymbol{u}}_a(t) = B_0[\boldsymbol{u}_a(t) - \hat{\boldsymbol{u}}_a(t)] = -\tilde{\Theta}(t)\boldsymbol{f}(\boldsymbol{\omega}, \boldsymbol{\sigma})$, and ν, c_3 and c_4 are positive constants.

Proof. It is straightforward to show that $\boldsymbol{\eta}(t)$ satisfies the differential equation

$$\ddot{\boldsymbol{\eta}}(t) + \lambda\dot{\boldsymbol{\eta}}(t) + \gamma\rho(t)B_m^{\top}PB_m\boldsymbol{\eta}(t) = \gamma\left[\dot{\rho}(t)B_m^{\top}P + \rho(t)B_m^{\top}PA_m\right]\tilde{\boldsymbol{e}}(t) + \lambda\boldsymbol{h}(t) + \dot{\boldsymbol{h}}(t)\,, \tag{32}$$

where we denote

$$\begin{aligned} \rho(t) &= \boldsymbol{f}^{\top}(\boldsymbol{\omega}, \boldsymbol{\sigma})\boldsymbol{f}(\boldsymbol{\omega}, \boldsymbol{\sigma}) \\ \boldsymbol{h}(t) &= \tilde{\Theta}^{\top}(t)\left[\frac{\partial \boldsymbol{f}}{\partial \boldsymbol{\omega}}\dot{\boldsymbol{\omega}}(t) + \frac{\partial \boldsymbol{f}}{\partial \boldsymbol{\sigma}}\dot{\boldsymbol{\sigma}}(t)\right], \end{aligned} \tag{33}$$

which are bounded as long as $\boldsymbol{\omega}(t)$ and $\boldsymbol{\sigma}(t)$ are bounded. In particular, there exist positive constants $\alpha_1,\ \alpha_2,\ \alpha_3$ such that $\|\rho(t)\|_{\mathcal{L}_\infty} \leq \alpha_1$, $\|\dot{\rho}(t)\|_{\mathcal{L}_\infty} \leq \alpha_2$ and $\|\boldsymbol{h}(t)\|_{\mathcal{L}_\infty} \leq \alpha_3$. Since all the terms in equation (32) are bounded functions in time, it can be considered as a second order linear equation with time varying coefficients in $\boldsymbol{\eta}(t)$. Although equation (32) is non-autonomous, it can still be concluded that the adaptation rate γ determines the frequency of $\boldsymbol{\eta}(t)$. Therefore, increasing γ increases the oscillations in the adaptive

signal $\boldsymbol{\eta}(t)$. On the other hand, λ determines the damping ratio. Therefore increasing λ suppresses the oscillations in the adaptive signal $\boldsymbol{\eta}(t)$.

Next we show that the peak value of $\boldsymbol{\eta}(t)$ can be decreased as desired by increasing the adaptation rate, when a proper value for the parameter λ is selected. Let $\alpha_0 \geq \rho(t)B_m^\top PB_m \geq c_0$, where c_0 is a positive constant. Denoting $a_0 = \frac{\alpha_0+c_0}{2}$, $E_1(t) = \dot{\rho}(t)B_m^\top P + \rho(t)B_m^\top PA_m$ and $E_2(t) = a_0\mathbb{I} - \rho(t)B_m^\top PB_m\Lambda$, we write the equation (32) in the following form

$$\ddot{\boldsymbol{\eta}}(t) + \lambda\dot{\boldsymbol{\eta}}(t) + \gamma a_0\boldsymbol{\eta}(t) = \gamma E_1(t)\tilde{\boldsymbol{e}}(t) + \gamma E_2(t)\boldsymbol{\eta}(t) + \lambda\boldsymbol{h}(t) + \dot{\boldsymbol{h}}(t)\,, \tag{34}$$

the solution of which is readily represented in the equivalent integral form

$$\begin{aligned}\boldsymbol{\eta}(t) = {} & \boldsymbol{\psi}(t)\begin{bmatrix}\boldsymbol{\eta}(0) & \dot{\boldsymbol{\eta}}(0)\end{bmatrix}^\top + \\ & \gamma\int_0^t \psi_2(t-\tau)[E_1(\tau)\tilde{\boldsymbol{e}}(\tau) + E_2(\tau)\boldsymbol{\eta}(\tau)]d\tau + \\ & \int_0^t [\psi_1(t-\tau) + \lambda\psi_2(t-\tau)]\boldsymbol{h}(\tau)d\tau\,,\end{aligned} \tag{35}$$

where $\boldsymbol{\psi}(t) = \begin{bmatrix}\psi_1(t) & \psi_2(t)\end{bmatrix}$ is the first row of the state transition matrix $e^{(A_c t)}$, where

$$A_c = \begin{bmatrix}0 & 1\\ -\gamma a_0 & -\lambda\end{bmatrix}.$$

Therefore, $\boldsymbol{\eta}(t)$ can be upper bounded as follows

$$\begin{aligned}\|\boldsymbol{\eta}(t)\|_{\mathcal{L}_\infty} \leq {} & e^{-\nu t}(\|\boldsymbol{\eta}(0)\| + \|\dot{\boldsymbol{\eta}}(0)\|) \\ + {} & \gamma\|\psi_2(t)\|_{\mathcal{L}_1}\|E_1(t)\tilde{\boldsymbol{e}}(t) + E_2(t)\boldsymbol{\eta}(t)\|_{\mathcal{L}_\infty} \\ + {} & \|\psi_1(t) + \lambda\psi_2(t)\|_{\mathcal{L}_1}\|\boldsymbol{h}(t)\|_{\mathcal{L}_\infty}\,,\end{aligned} \tag{36}$$

where $\nu = \min Re(\lambda(A_c))$. Solving the inequality for (36) for $\|\boldsymbol{\eta}(t)\|_{\mathcal{L}_\infty}$ and substituting for $\|\tilde{\boldsymbol{e}}(t)\|_{\mathcal{L}_\infty}$ and $\|E_1(t)\|_{\mathcal{L}_\infty}$, we obtain

$$\begin{aligned}&[1 - \gamma\|\psi_2(t)\|_{\mathcal{L}_1}\|E_2(t)\|_{\mathcal{L}_\infty}]\,\|\boldsymbol{\eta}(t)\|_{\mathcal{L}_\infty} \\ &\leq e^{-\nu t}(\|\boldsymbol{\eta}(0)\| + \|\dot{\boldsymbol{\eta}}(0)\|) \\ &+c_1(\alpha_2\|B_m^\top P\| + \alpha_1\|B_m^\top PA_m\|)\sqrt{\gamma}\|\psi_2(t)\|_{\mathcal{L}_1} \\ &+\alpha_3\|\psi_1(t) + \lambda\psi_2(t)\|_{\mathcal{L}_1}\,.\end{aligned}$$

Since $c_0 \leq \rho(t)B_m^\top PB_m\Lambda \leq \alpha_0$ we have

$$\|E_1(t)\|_{\mathcal{L}_\infty} = a_0 - c_0 = \frac{\alpha_0 - c_0}{2}.$$

On the other hand, it can be shown (see[10] for details) that the $\mathcal{L}_1$ norm of $\psi_2(t)$ is minimized when $\lambda_0 = 2\sqrt{\gamma a_0}$ and is equal to $\frac{1}{\gamma a_0}$. Therefore the left hand side coefficient can be evaluated as follows

$$1 - \gamma\|g_{2i}(t)\|_{\mathcal{L}_1}\|a_0\mathbb{I} - \rho(t)B_0^\top PB_0\Lambda\|_{\mathcal{L}_\infty} = \frac{2c_0}{\alpha_0 + c_0}\,. \tag{37}$$

For the same λ_0, we have

$$\|\psi_1(t) + \lambda_0\psi_2(t)\|_{\mathcal{L}_1} \leq \frac{4}{\sqrt{\gamma a_0}}.$$

Substituting these results into (37) we obtain the inequality (31) with

$$\begin{aligned}c_3 &= \frac{a_0}{c_0}\,[\|\boldsymbol{\eta}(0)\| + \|\dot{\boldsymbol{\eta}}(0)\|] \\ c_4 &= \frac{4\alpha_3\sqrt{a_0}}{c_0} + \frac{c_1(\alpha_1\|B_0^\top PA_m\| + \alpha_2\|B_0^\top P\|)}{c_0}\,.\end{aligned}$$

This concludes the proof. □

Lemma V.3 implies that the control deficiency estimation error signal $B_0^{-1}\boldsymbol{\eta}(t)$ can be made as close to a decaying exponential $c_3e^{-\nu t}$ as desired by increasing the adaptation rate in the presented adaptive scheme. Hence the estimate $\hat{\boldsymbol{u}}_a(t)$ can be used in the closed loop as a recovery option in the loss-of-control situation.

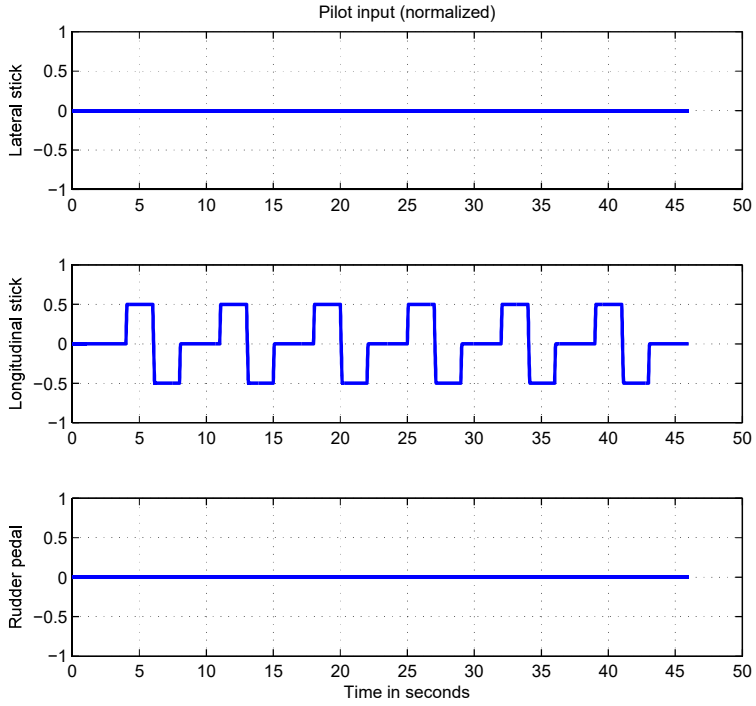

Figure 2. Pilot's normalized input.

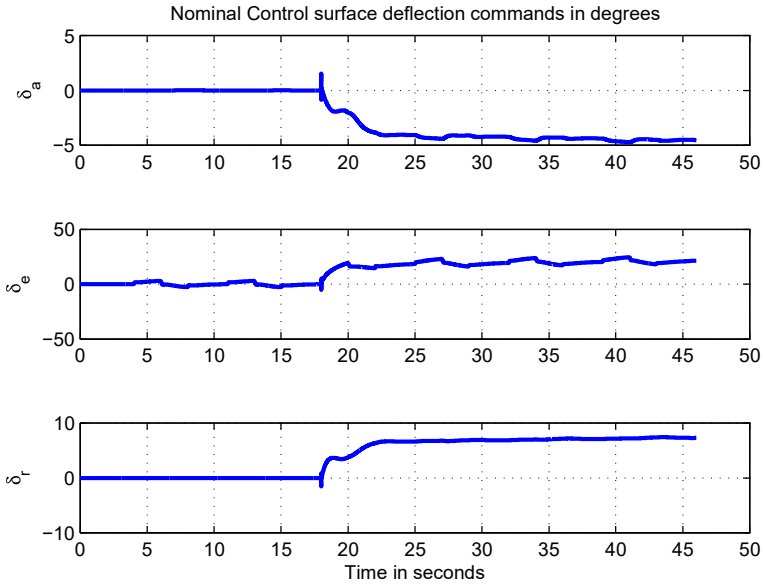

Figure 3. Nominal control signal generated by the PI controller, failure initiated at $t = 18$ *sec*.

VI. Simulation results

In this section we present simulation results for the developed detection and mitigation algorithm using Generic Transport Model (GTM).[2,7]

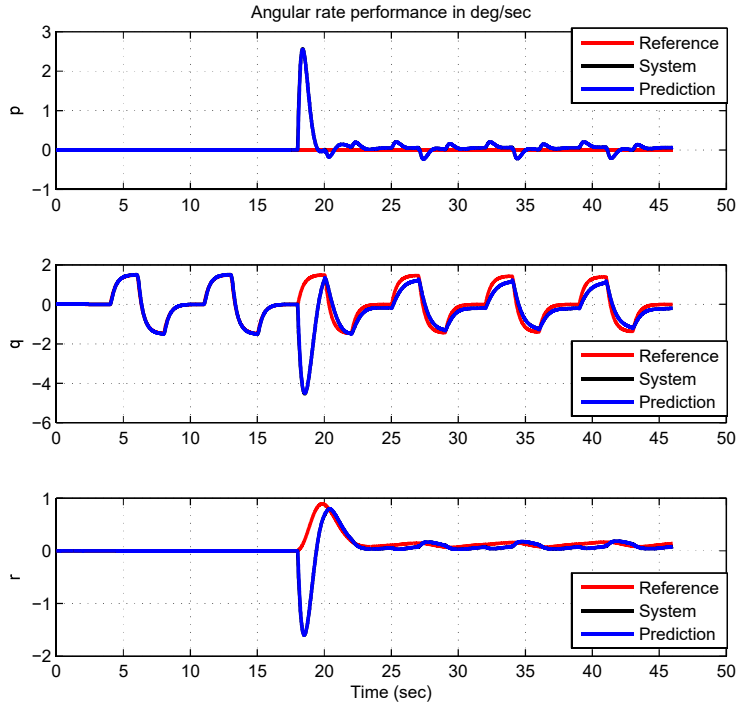

Figure 4. Performance of the nominal controller in the presence of uncertainties at $t = 18$ sec.

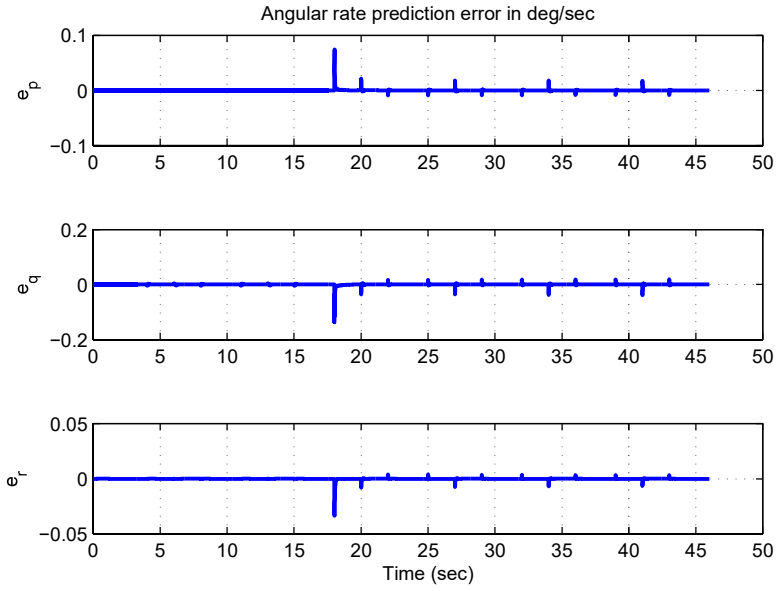

Figure 5. Angular rates prediction errors.

The nominal aircraft is in the steady level flight at an altitude of 15000 ft and speed of 0.65 M. The pilot's input is displayed in Figure 2 and is a series of doublet commands in the pitch channel. The nominal proportional-integral control is designed with frequencies 3.5 2.5 2.0 rad/sec respectively in roll, pitch and

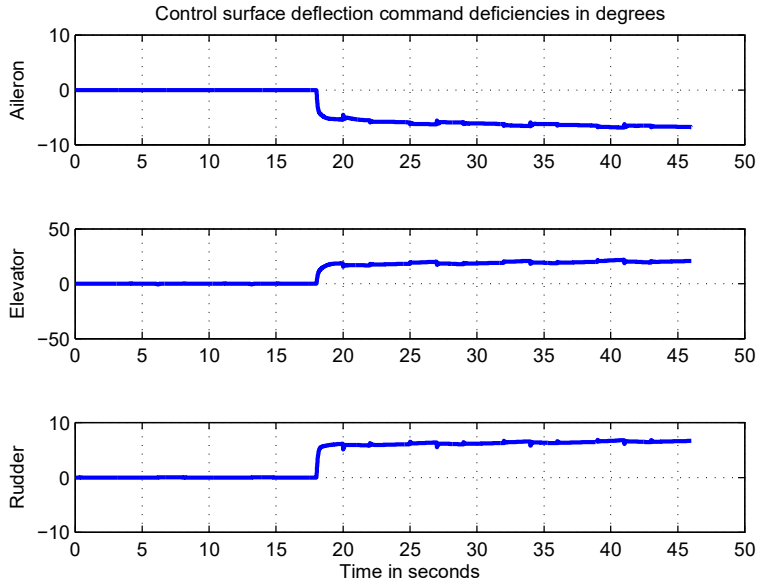

Figure 6. Control deficiency signal in the open loop.

yaw channels and with the damping ratio of 0.707 in all channels. The aircraft experiences a left horizontal tail damage and loss of left elevator at $t = 18$ *sec*. Although the aircraft is still stable, it can be observed from Figure 4 that the nominal controller cannot provide adequate tracking. Figure 4 also displays the performance of the prediction model, which is practically indistinguishable from the operating aircraft for the chosen parameters $\gamma = 5000$ and $\lambda = 184$. To give a better understanding of the prediction error we present it in Figure 5, where small peaks are attributed to the parameter changes at $t = 18$ *sec* and discontinuities in the pilot's inputs. The estimates of the control signal deficiencies are presented in Figure 6. It can be observed that these estimates experience large changes in magnitude right after the damage occurs signaling the loss-of-control situation.

In the next simulation we close the loop with the adaptive estimates of control deficiencies at $t = 32$ *sec*. It can be observed from Figure 7 that the tracking of the reference model is smoothly recovered, implying that these adaptive signals are viable options for the pilot to save the situation. Figure 8 displays the applied control signal with the adaptive estimates in the loop. It can be observed that this signal is not affected with the high frequency oscillations and big excursions.

VII. Conclusion

We have presented an adaptive prediction based algorithm for aircraft loss-of-control detection, which also provides an optional solution to the pilot. The prediction system does not interact with the aircraft flight control system and can be implemented in the onboard computer during the entire flight. Unlike the online parameter identification methods the algorithm does not require any additional maneuver. The loss-of-control situation is detected whenever the algorithm generates nonzero (or exceeding the specified threshold) control deficiency signal. It has been shown that the state prediction and its derivative converge to the true values fast, and the generated adaptive signals are smooth and oscillation free. When the control deficiency is included in the closed loop, the tracking of the reference model is smoothly recovered.

References

[1]C. M. Belcastro and J. V. Foster, "Aircraft Loss-of-Control Accident Analysis," *AIAA paper AIAA-2010-8004*, 2010.

[2]T. Jordan and W. Langford, "Development of a Dynamically Scaled Generic Transport Model Testbed for Flight Research Experiments," *In Proc. AUVSI Unmannded Systems North America, Arlington, VA*, 2004.

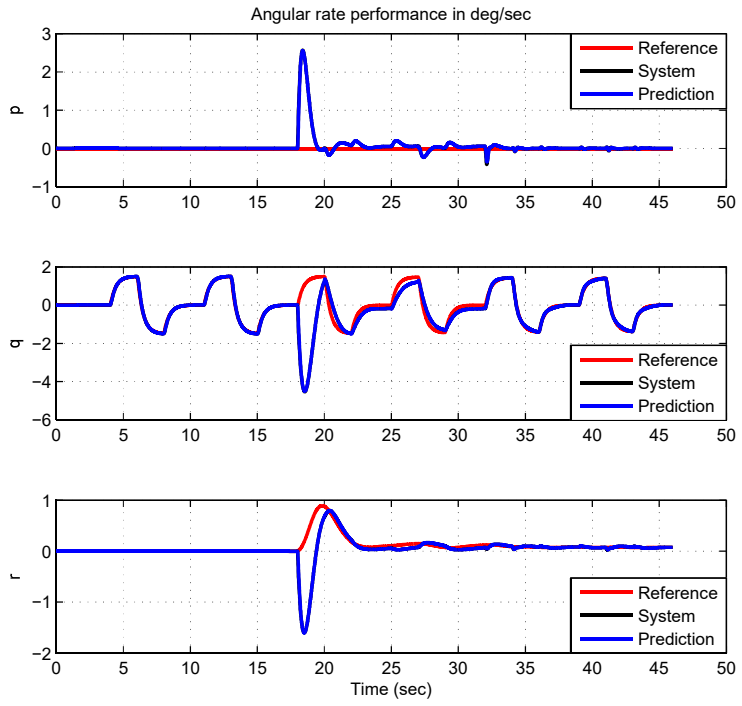

Figure 7. Performance of the aircraft with the control deficiency in the loop $t = 32$ *sec*.

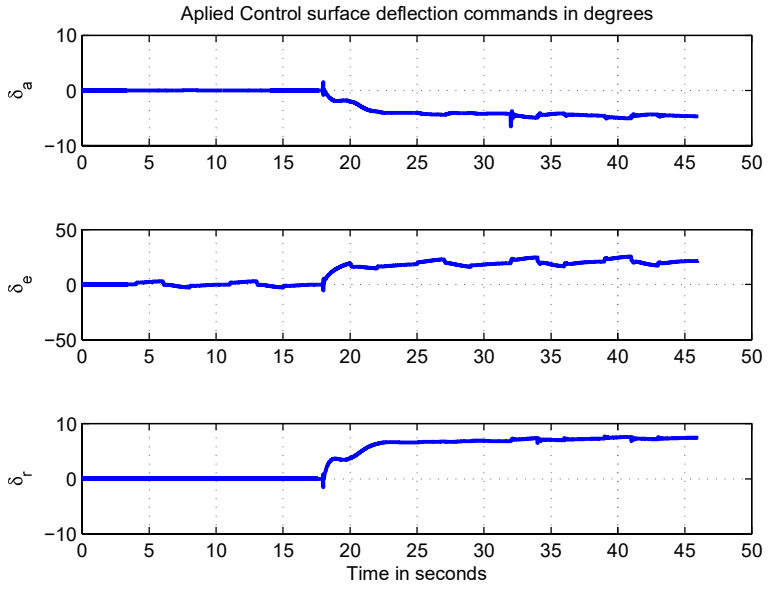

Figure 8. Applied control signal control deficiency in the loop $t = 32$ *sec*.

[3]H. Khalil, *Nonlinear Systems, Third Edition*. Prentice Hall, New Jersey, 2002.

[4]H. G. Kwatny, J.-E. T. Dongmo, B.-C. Vhang, G. Bajpai, M. Yasar, and C. Belcastro, "Aircraft Accident Prevention: Loss-of-Control Analysis," *AIAA paper AIAA-2009-6256*, 2009.

[5]L. Ma and Y. Zhang, "Fault Detection and Diagnosis for GTM UAV with Dual Unscented Kalman Filter," *AIAA paper*

AIAA-2010-7884, 2010.

[6]E. Morelli and M. Smith, "Real-Time Dynamic Modeling: Data Information Requirements and Flight-Test Results," *Journal of Aircraft*, vol. 46, pp. 1894–1905, 6 2009.

[7]A. Murch and J. Foster, "Recent NASA Research on Aerodynamic Modeling of Post-Stall and Spin Dynamics of Large Transport Airplanes," *In Proc. 45th AIAA Aerospace Sciences Meeting and Exhibit, Reno, NV*, 2007.

[8]R. Pandita, A. Chakraborty, P. Seiler, and G. Balas, "Reachability and Region of Attraction Analysis Applied to GTM Flight Envelope Assessment," *AIAA paper AIAA-2009-6258*, 2009.

[9]M. Ruschmann and J.-Y. Shin, "Actuator Fault Diagnosis Using Two-Stage Extended Kalman Filters," *AIAA paper AIAA-2010-7703*, 2010.

[10]V. Stepanyan and K. Krishnakumar, "Modified Reference Model MRAC Has Guaranteed Input-Output Performance," *The International Journal of Control*, Submitted 2010.

[11]J. Sun and S. Joshi, "An Indirect Adaptive Control Scheme in the Presence of Actuator/ Sensor Failures," *AIAA paper AIAA-2009-5740*, 2009.

[12]J. E. Wilborn and J. V. Foster, "Defining Comertial Loss-of-Control: A Quatitative Approach," *AIAA paper AIAA-2004-4811*, 2004.